

Frequency Shifts of the Internal Phonon Modes in $\text{La}_{0.7}\text{Ca}_{0.3}\text{MnO}_3$

K. H. Kim,* J. Y. Gu, H. S. Choi, G. W. Park, and T. W. Noh†

Department of Physics, Seoul National University, Seoul 151-742, Korea
(Received 14 December 1995; revised manuscript received 11 June 1996)

Infrared reflectivity spectra were measured for a polycrystalline $\text{La}_{0.7}\text{Ca}_{0.3}\text{MnO}_3$ sample. The internal phonon modes, i.e., the bending and stretching modes, of the MnO_6 octahedra show significant frequency shifts near the Curie temperature T_C . The frequency shifts of the internal phonon modes were found to have a linear relationship with the excess lattice expansion above T_C , which deviates from a prediction of the Grüneisen law. A strong electron-phonon coupling and a crossover from small to large polaronic states are attributed to the observed frequency shifts. [S0031-9007(96)01066-6]

PACS numbers: 78.30.-j, 63.80.Kr, 72.15.Gd, 75.80.+q

Recently, perovskite $\text{La}_{1-x}\text{A}_x\text{MnO}_3$ (A is a divalent element such as Sr and Ca) has attracted much attention due to its large negative magnetoresistance. For a broad range of doping concentration, i.e., $0.2 \leq x \leq 0.5$, this material has a ferromagnetic (FM) ordering at T_C [1]. Interestingly, a typical temperature dependent resistivity curve of $\text{La}_{1-x}\text{A}_x\text{MnO}_3$ shows an insulating behavior above T_C and a metallic behavior below T_C .

The coexistence of the FM ordering and the metallic behavior has been traditionally explained within a framework of the double exchange (DE) model [2], which is based on a strong exchange interaction between itinerant e_g and localized t_{2g} electrons. However, a recent calculation by Millis *et al.* indicated that the DE model alone cannot explain resistivity and magnetoresistance effects quantitatively [3,4]. In addition to the DE physics, they proposed that a lattice polaron due to a strong electron-phonon interaction plays an important role. Especially, they claimed that the lattice distortion due to the Jahn-Teller splitting of the outer Mn d level is important. There have been lots of experimental works [5,6] which suggest importance of the electron-lattice coupling in the manganese oxide, but a clear connection to the polaron effect is still lacking.

Infrared (IR) phonon spectra are sensitive to local lattice distortions [4,7]. Okimoto *et al.* [8] measured optical spectra of a single crystal $\text{La}_{1-x}\text{Sr}_x\text{MnO}_3$, but its phonon spectra were not studied in detail. In this Letter, we report our investigations on IR spectra of a polycrystalline $\text{La}_{0.7}\text{Ca}_{0.3}\text{MnO}_3$ (LCMO) sample. While the sample enters from a paramagnetic insulating state into a FM metallic state, the transverse optic (TO) phonon frequencies for the bending and stretching modes increase by 10 and 20 cm^{-1} , respectively. These phonon frequency shifts will be compared with predictions of a model by Lee and Min [9], which combines the DE interaction and the lattice polaron. This work indicates that the electron-phonon coupling plays an important role in the lattice dynamics of the manganese oxide.

A polycrystalline LCMO sample was synthesized by a standard solid-state reaction method [10]. After calcining and grinding repeatedly, resulting powder was pressed into

a pellet under 200 MPa using a cold isostatic pressing, and sintered. Sintering condition was optimized to get a sample of a high density, i.e., 98% of its theoretical value. The sample was finally annealed at 1100 °C for 24 h in a flowing oxygen atmosphere. A powder x-ray diffraction study showed that the LCMO sample is a single phase with a pseudocubic perovskite structure. The inset of Fig. 1 shows a magnetization curve which was measured under a magnetic field of 100 Oe after a field cooling: the LCMO sample has a FM ordering at $T_C \approx 250$ K. The inset also shows that temperature dependent dc resistivity, $\rho(T)$, decreases sharply near T_C .

Before IR reflectivity measurements, the LCMO sample was polished up to 0.3 μm . Near normal incidence reflectivity spectra were measured using a Fourier-transform IR spectrophotometer between 50 and 5000 cm^{-1} , and a grating spectrophotometer between 3000 and 53 000 cm^{-1} . Temperature of the sample was varied with a liquid He-cooled cryostat.

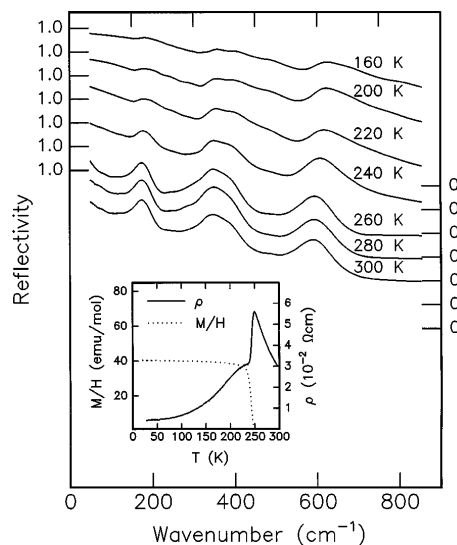


FIG. 1. Infrared reflectivity spectra of the $\text{La}_{0.7}\text{Ca}_{0.3}\text{MnO}_3$ sample. The inset displays temperature dependent resistivity and magnetization curves. The magnetization was measured at 100 Oe after a field cooling.

Figure 1 shows temperature dependent IR reflectivity spectra. At 300 K, the spectrum shows three main phonon bands. For a cubic perovskite [11], twelve optic phonons for $\mathbf{q} = 0$ transform as the $(3F_{1u} + F_{2u})$ triply degenerate irreducible representations of the $O_h(m3m)$ point group. The F_{2u} mode is IR inactive, and three F_{1u} modes are IR active. The F_{1u} phonon modes are called “external,” “bending,” or “stretching” modes, depending on the types of collective motions. The external mode, located around 170 cm^{-1} , represents a vibrating motion of the La (Ca) ions against the MnO_6 octahedra. The bending mode, located around 330 cm^{-1} , reflects an internal motion of the Mn and O ions located along a particular direction against the other oxygen ions in a plane perpendicular to the direction. This mode is strongly affected by a change in the Mn-O-Mn bond angle. The stretching mode, located near 580 cm^{-1} , corresponds to an internal motion of the Mn ion against the oxygen octahedron and is sensitive to the Mn-O bond length [11].

Optical conductivity, $\sigma(\omega)$, was obtained from the Kramers-Kronig transformation of the reflectivity R . For a high frequency extrapolation, R above 53000 cm^{-1} was assumed to be constant up to 35 eV and have ω^{-4} dependence above 35 eV . For a low frequency extrapolation, the Hagen-Rubens relation was used: $R \approx 1 - \sqrt{2\omega\rho_{\text{IR}}}/\pi$, where ρ_{IR} is the dc resistivity obtained by extrapolating the IR data. It is found that ρ_{IR} is smaller than the measured ρ by 1 or 2 orders of magnitude. A similar behavior was observed in the microwave region and attributed to tunneling across intergranular barriers [12]. We changed the annealing conditions and obtained LCMO samples with ρ between 30 and 300 m Ω cm. However, these samples had almost the same IR reflectivities, suggesting that ρ is strongly influenced by intergranular conduction and that ρ_{IR} reveals a more intrinsic property of LCMO. A detailed study on this effect will be published elsewhere [13].

The spectra of $\sigma(\omega)$ are shown in Fig. 2. Three strong TO phonon peaks corresponding to the external, bending, and stretching modes are observed at ω_{T1} , ω_{T2} , and ω_{T3} , respectively. At a low frequency region, there is a contribution from free carriers. As T is lowered, the free carrier contribution screens the external phonon mode. The line shapes of the phonon peaks are quite asymmetric, indicating that electron-phonon coupling is strong in the LCMO sample. In Fig. 2, it is important to note that ω_{T2} and ω_{T3} change as T decreases. As T is lowered, both ω_{T2} and ω_{T3} clearly shift to higher frequencies. The dielectric function, $\tilde{\epsilon}(\omega)$, of LCMO was modeled with a Drude function and four Lorentz oscillators [14],

$$\tilde{\epsilon}(\omega) = \epsilon_{\infty} - \frac{\omega_p^2}{(\omega^2 + i\omega/\tau)} + \sum_{j=1}^4 \frac{S_j}{\omega_{Tj}^2 - \omega^2 - i\gamma_j\omega}, \quad (1)$$

where ϵ_{∞} is high frequency limit of $\tilde{\epsilon}(\omega)$. ω_p and τ are plasma frequency and relaxation time of free carriers, respectively. And, S_j , ω_{Tj} , and γ_j are the strength, frequency, and width of the j th Lorentz oscillator, respectively, where $j = 1-3$ represent three phonon modes and $j = 4$ a mid-IR absorption band.

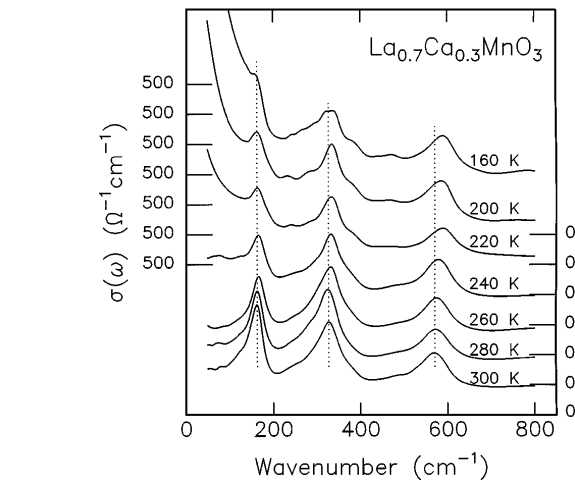


FIG. 2. Optical conductivity spectra of the LCMO sample at various temperatures. The room temperature positions of TO phonon frequencies are shown as dotted lines. As temperature decreases, the TO phonon frequencies of the bending and stretching modes increase significantly.

ers, respectively. And, S_j , ω_{Tj} , and γ_j are the strength, frequency, and width of the j th Lorentz oscillator, respectively, where $j = 1-3$ represent three phonon modes and $j = 4$ a mid-IR absorption band.

The TO phonon frequencies obtained from the fitting are shown in Fig. 3. While ω_{T1} is nearly independent of T , ω_{T2} and ω_{T3} change notably around T_C . For the bending mode, ω_{T2} is 327 cm^{-1} at 300 K and increases to 337 cm^{-1} at 160 K, resulting in a shift of 10 cm^{-1} . For the stretching mode, ω_{T3} changes from 573 cm^{-1} at 300 K to 593 cm^{-1} at 160 K, resulting in a shift of 20 cm^{-1} . These

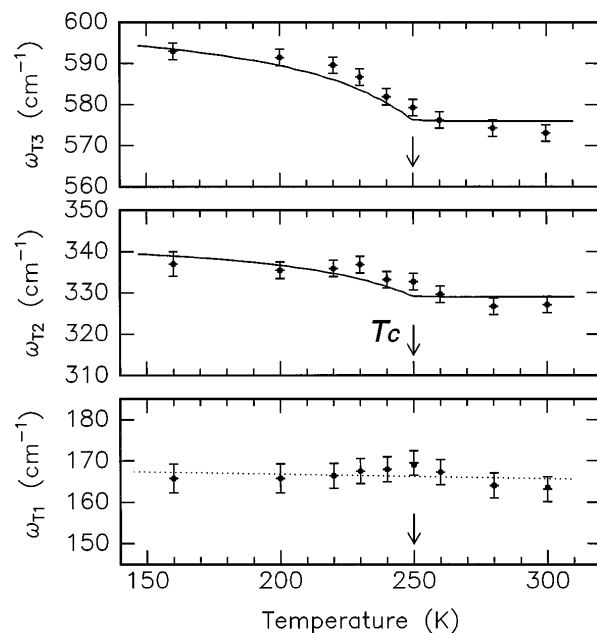


FIG. 3. TO phonon frequencies at various temperatures. The solid lines for ω_{T2} and ω_{T3} are predictions of a model by Lee and Min [9], which considers polaron transport and lattice dynamics.

frequency shifts indicate that the Mn-O-Mn bond angle and the Mn-O distance change near the metal-insulator (MI) transition.

Figure 4 shows the temperature dependent lattice constant, $a(T)$, which was measured from x-ray diffraction studies. Within our experimental resolution, LCMO remained in a pseudocubic phase above and below T_C . The increase of $a(T)$ between 80 and 300 K is about 0.005 Å, corresponding to a length change of $\sim 0.13\%$. Note that $a(T)$ changes significantly near T_C . A maximum of thermal expansivity, $d[a(T)/a(160\text{ K})]/dT$, is located near 245 K, suggesting that the change in the lattice constant is closely related to the MI transition. To see this effect more clearly, a thermal lattice expansion due to anharmonicity, $a_{\text{ah}}(T)$, was evaluated with the Grüneisen law with its Debye temperature of 530 K [15] and drawn as a dotted line in Fig. 4. There exists an excess lattice expansion, $a_{\text{ex}} \equiv (a - a_{\text{ah}})$, above T_C . A similar effect was observed in $\text{La}_{0.6}\text{Y}_{0.07}\text{Ca}_{0.33}\text{MnO}_3$ and attributed to the polaron effect by Ibarra *et al.* [5].

As shown in Fig. 5, a normalized change of the lattice constant, $\Delta a_{\text{ex}}/a \equiv [a_{\text{ex}}(T) - a_{\text{ex}}(160\text{ K})]/a(160\text{ K})$, increases drastically near T_C and starts to saturate near 270 K. Normalized changes of the bending and stretching phonon peaks, $\Delta\omega_{Tj}/\omega_{Tj} \equiv [\omega_{Tj}(160\text{ K}) - \omega_{Tj}(T)]/\omega_{Tj}(160\text{ K})$, are also plotted with solid squares and circles, respectively. It is quite clear that the $\Delta\omega_{T2}$ and $\Delta\omega_{T3}$ are almost linearly proportional to Δa_{ex} . And, it can also be inferred that a_{ah} does not affect much on the frequency shifts. Interestingly, the relative changes of ω_{T2} and ω_{T3} are much larger than that of a_{ex} : compared to the value of 0.04% in $\Delta a_{\text{ex}}/a$, $\Delta\omega_{Tj}/\omega_{Tj}$ ($j = 2$ and 3) gives a large amount, i.e., about 3%.

A second-order magnetic phase transition is accompanied by a discontinuity in the thermal expansion coefficient

α near T_C , and $\Delta\omega_{T2}$ and $\Delta\omega_{T3}$ might be related to such an effect. For example, a similar magnetoelastic behavior was observed in EuO, which also shows a magnetoresistance near T_C [16]. The Ehrenfest relation predicts that $\Delta\alpha = (\Delta C_p/3T_C V)(\partial T_C/\partial P)$, where C_p and V are a specific heat and a volume of the sample, respectively. The pressure dependence of T_C , $(\partial T_C/\partial P)$, is found to be quite large (i.e., 16 K/GPa) [17] for this manganese oxide. From the known values of $\Delta C_p \approx 40\text{ J/K mol}$ [18], it is estimated that $\Delta\alpha \approx 2.4 \times 10^{-5}\text{ K}^{-1}$, which is comparable to the expansivity observed in Fig. 4. However, a magnetoelastic effect cannot be a main source for the phonon frequency shifts in LCMO for the following three reasons: first, the shape of α in Fig. 4 cannot be fitted with an observed λ -like shape of C_p/T by Ramirez *et al.* [18]. Second, the change in M , shown in the inset of Fig. 1, occurs in a very narrow temperature region near T_C , so a typical dependence between $\Delta V/V$ and M (such as $\Delta V/V \propto M^2$) cannot be satisfied. Third, the magnitude of $\Delta\omega_{Tj}$ observed in LCMO is larger by 1 or 2 orders of magnitude than that in other materials with a similar magnitude for $\Delta\alpha$ [19].

The anomalously large $\Delta\omega_{Tj}$ near the MI transition suggests that there is a strong electron-phonon coupling in LCMO [20]. And, it is quite possible that a formation of a local lattice distortion, called a "polaron," results in the large $\Delta\omega_{Tj}$. Recently, Lee and Min [9] investigated polaron transport and lattice dynamics using a model with a DE Hamiltonian and an electron-phonon interaction. In the insulating region (i.e., $T \geq T_C$) a small polaron is formed. In the metallic region, the elementary excitation becomes a large polaron due to an increase in the polaron bandwidth, $\gamma(T) \equiv \langle \cos(\theta/2) \rangle$, which is a thermodynamic average of the cosine of the angle between the directions

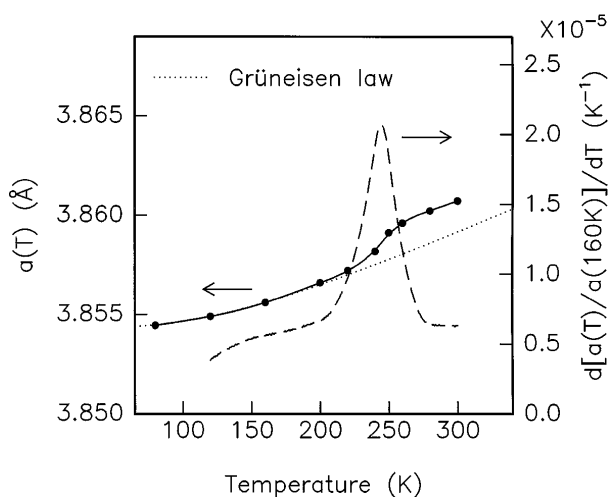


FIG. 4. The temperature dependent lattice constant of $\text{La}_{0.7}\text{Ca}_{0.3}\text{MnO}_3$. A thermal expansion curve expected from the Grüneisen law is drawn as a dotted line. The dashed line shows thermal expansivity normalized with respect to the value at 160 K, i.e., $d[a(T)/a(160\text{ K})]/dT$.

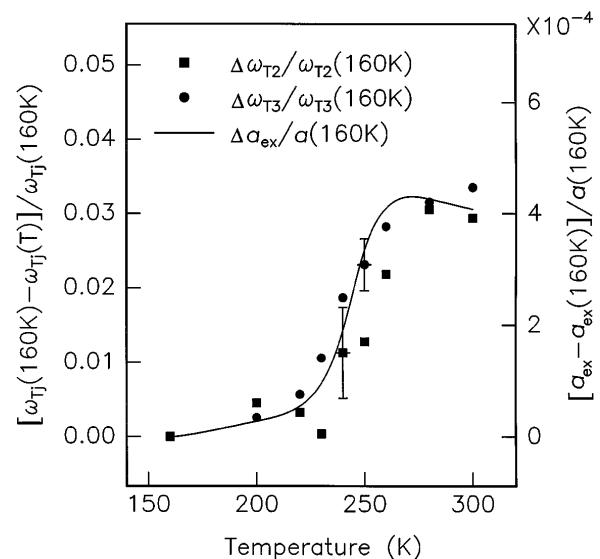


FIG. 5. Relative changes of TO phonon frequencies and excess lattice expansion. The solid squares and circles represent relative changes of ω_{T2} and ω_{T3} , respectively. Note that the frequency shifts are proportional to the excess lattice expansion.

of the neighboring spins. Then, the phonon frequency will shift due to the changes in the electron screening,

$$\tilde{\omega}_q^2(\omega) \approx \omega_q^2 - 2\omega_q|M_q|^2 \frac{1}{\gamma(T)} \sum_{\vec{k}} \frac{n_{\vec{k}} - n_{\vec{k}+\vec{q}}}{t_{\vec{k}+\vec{q}} - t_{\vec{k}}}, \quad (2)$$

where M_q is the electron-phonon coupling constant, and $t_{\vec{k}}$ and $n_{\vec{k}}$ are the transfer integral and the number operator in the \vec{k} space, respectively. Since the summation term is almost temperature independent, Eq. (2) can be approximated as $\tilde{\omega}_q \approx \omega_q[1 - \beta/\gamma(T)]^{1/2}$, where β is a nearly temperature independent parameter [21].

Using the temperature dependent $\gamma(T)$ predicted by a mean field theory [22], the experimental values of $\Delta\omega_{T2}$ and $\Delta\omega_{T3}$ were fitted with $\beta \approx 0.14$ and $T_C \approx 250$ K. As shown in Fig. 3, the theoretical predictions can explain the observed phonon frequency shifts quite well, indicating that the polaron plays an important role in the MI transition of LCMO.

In the polaronic picture, the local lattice distortion due to the strong electron-phonon coupling can transfer from one site to another, so crystal structure remains nearly cubic. Since the external phonon mode will not be affected much by the local distortion, the change in $\Delta\omega_{T1}$ will be negligible. Moreover, the local lattice distortion might change average lattice constant, which provides a qualitative explanation for the scaling between $\Delta a_{ex}/a$ and $\Delta\omega_{Tj}/\omega_{Tj}$ ($j = 2$ and 3). A further study is required to explain the scaling behavior quantitatively. It should also be noted that the dynamic Jahn-Teller distortion, suggested by Millis *et al.*, is essentially a form of polarons. But, it is still required to check whether the observed frequency shifts in the bending and stretching modes are related to the specific distortion.

In summary, we measured IR phonon spectra of a polycrystalline $\text{La}_{0.7}\text{Ca}_{0.3}\text{MnO}_3$. Both the bending and stretching modes of the MnO_6 octahedron show significant frequency shifts near the MI transition, which are explained in terms of a polaron model.

We would like to acknowledge Professor S.I. Lee, B.I. Min, and Y.H. Jeong for their useful discussions. This work was financially supported by the Ministry of Education through the Basic Science Research Institute Program No. BSRI-95-2416 and by the Korea Science and Engineering Foundation through the RCDAMP at Pusan National University.

*Electronic address: khkim@phy.snu.ac.kr

†Electronic address: twnoh@phy.snu.ac.kr

[1] G.H. Jonker and J.H. van Santen, *Physica (Utrecht)* **16**, 337 (1950).

- [2] C. Zener, *Phys. Rev.* **82**, 403 (1951); P. W. Anderson and H. Hasegawa, *ibid.* **100**, 675 (1955); P. G. de Gennes, *ibid.* **118**, 141 (1960).
- [3] A. J. Millis, P. B. Littlewood, and B. I. Shraiman, *Phys. Rev. Lett.* **74**, 5144 (1995).
- [4] A. J. Millis, *Phys. Rev. B* **53**, 8434 (1996); A. J. Millis, B. I. Shraiman, and R. Mueller, *Phys. Rev. Lett.* **77**, 175 (1996).
- [5] M. R. Ibarra *et al.*, *Phys. Rev. Lett.* **75**, 3541 (1995).
- [6] H. Y. Hwang *et al.*, *Phys. Rev. Lett.* **75**, 914 (1995); P. G. Radaelli *et al.*, *Phys. Rev. Lett.* **75**, 4488 (1995).
- [7] R. T. Harley, in *Electron-Phonon Interaction and Phase Transitions*, edited by T. Riste (Plenum, New York, 1977), and references therein; J. B. Goodenough *et al.*, *Phys. Rev.* **124**, 373 (1961).
- [8] Y. Okimoto *et al.*, *Phys. Rev. Lett.* **75**, 109 (1995).
- [9] J. D. Lee and B. I. Min (unpublished).
- [10] J. Y. Gu *et al.*, *J. Appl. Phys.* **78**, 6151 (1995).
- [11] M. D. Fontana *et al.*, *J. Phys. C* **16**, 483 (1984); T. Arima and Y. Tokura, *J. Phys. Soc. Jpn.* **64**, 2488 (1995).
- [12] J. S. Ramachandran *et al.*, *Solid State Commun.* **96**, 127 (1995).
- [13] K. H. Kim *et al.* (unpublished).
- [14] Because of the asymmetric line shape, the Fano function or the rotated Lorentzian function provides a better fitting for each phonon mode. Refer to C. C. Homes *et al.*, *Can. J. Phys.* **73**, 663 (1995), and references therein.
- [15] J. Tanaka and T. Mitsuhashi, *J. Phys. Soc. Jpn.* **53**, 24 (1984); J. M. Ziman, *Principles of the Theory of Solids* (Cambridge University Press, New York, 1972).
- [16] B. E. Argyle and N. Miyata, *Phys. Rev. B* **171**, 555 (1968); T. Nakajima, *J. Phys. Soc. Jpn.* **19**, 520 (1964).
- [17] J. J. Neumeier *et al.*, *Phys. Rev. B* **52**, R7006 (1995); H. Y. Hwang *et al.*, *ibid.* **52**, 15 046 (1995).
- [18] A. P. Ramirez *et al.*, *Phys. Rev. Lett.* **76**, 3188 (1996).
- [19] For example, an antiferromagnetic ordering in KNiF_3 gives a decrease in its expansion coefficient of about $1 \times 10^{-5} \text{ K}^{-1}$, but only 1 cm^{-1} shift of the bending mode. Refer to K. Sintani *et al.*, *J. Phys. Soc. Jpn.* **25**, 99 (1968).
- [20] When neutral atoms are vibrating in a periodic harmonic potential, the phonon frequency depends on the lattice constant as $\omega_T^2 \propto a^{-3}$. Our frequency shifts are unusually large compared with relative changes of lattice 0.13%: ω_{Tj} ($j = 2$ and 3) roughly depends on a as $\omega_{Tj} \propto a^{-n}$ with $n \geq 20$. In materials with CuO_2 plane, remarkably large changes of ω_{Tj} against a was also observed ($\omega_T \propto a^{-n}$ with $n \approx 7$) and attributed to a direct coupling of the phonon mode with charge transfer electronic excitation between O and Cu. See S. Tajima *et al.*, *Phys. Rev. B* **43**, 10496 (1991).
- [21] G. D. Mahan, *Many-Particle Physics* (Plenum, New York, 1990).
- [22] K. Kubo and N. Ohata, *J. Phys. Soc. Jpn.* **33**, 21 (1972).